Chem Soc Rev

Aerobic biological methane oxidation

Journal:	*Chemical Society Reviews*
Manuscript ID	CS-REV-10-2020-001291.R1
Article Type:	Review Article
Date Submitted by the Author:	14-Dec-2020
Complete List of Authors:	Koo, Christopher; Northwestern University, Molecular Biosciences and Chemistry Rosenzweig, Amy; Northwestern University, Molecular Biosciences and Chemistry

ARTICLE

Biochemistry of aerobic biological methane oxidation

Christopher W. Koo [a] and Amy C. Rosenzweig [a]*

Received 00th October 2020,
Accepted 00th October 2020

DOI: 10.1039/x0xx00000x

Methanotrophic bacteria represent a potential route to methane utilization and mitigation of methane emissions. In the first step of their metabolic pathway, aerobic methanotrophs use methane monooxygenases (MMOs) to activate methane, oxidizing it to methanol. There are two types of MMOs: a particulate, membrane-bound enzyme (pMMO) and a soluble, cytoplasmic enzyme (sMMO). The two MMOs are completely unrelated, with different architectures, metal cofactors, and mechanisms. The more prevalent of the two, pMMO, is copper-dependent, but the identity of its copper active site remains unclear. By contrast, sMMO uses a diiron active site, the catalytic cycle of which is well understood. Here we review the current state of knowledge for both MMOs, with an emphasis on recent developments and emerging hypotheses. In addition, we discuss obstacles to developing expression systems, which are needed to address outstanding questions and to facilitate future protein engineering efforts.

1. Introduction

During an era of unprecedented climate change, increasing atmospheric methane concentrations are a constant source of concern and debate.[1,2] Anthropogenic methane emissions from oil and gas production, livestock, and agriculture threaten to fuel unstoppable global warming if left unchecked. Methane is the second most abundant greenhouse gas after carbon dioxide and accounts for at least 25% of current global warming. Moreover, its superior heat-trapping capacity confers a global warming potential 84 times that of carbon dioxide over a 20-year period. The effectiveness of methane as a greenhouse gas combined with its ~10 year lifetime means that immediate small reductions in atmospheric methane can have a large impact on climate change.[3]

Methane can be converted to desirable fuels and chemicals, which could simultaneously mitigate global warming and meet increasing energy demands.[4] However, activation of the 105 kcal mol^{-1} methane C-H bond[5] presents a significant challenge. Industrial methods rely on the conversion of methane and water to a mixture of carbon monoxide and hydrogen (syngas) followed by Fischer-Tropsch synthesis of longer-chain hydrocarbons.[6] This technically complex and expensive process must be carried out in large refineries to capture economies of scale.[4] The high capital expenses combined with the abundance of methane in remote locations have renewed interest in biological methane activation,

[a] Departments of Molecular Biosciences and of Chemistry, Northwestern University, Evanston, IL 60208, USA. Email: amyr@northwestern.edu

Christopher W. Koo

Christopher W. Koo received a BS in biochemistry from the University of California, Los Angeles. He is currently a PhD candidate in the Interdisciplinary Biological Sciences program (IBiS) at Northwestern University. In the Rosenzweig lab, his thesis work is focused on the structure and function of particulate methane monooxygenase in lipid nanodiscs using cryo-electron microscopy and cell-free protein synthesis. He is a former trainee of the NIH-funded Molecular Biosciences Training Program.

Amy C. Rosenzweig

Amy C. Rosenzweig received a BA in chemistry from Amherst College and a PhD in inorganic chemistry from Massachusetts Institute of Technology. After postdoctoral research at Harvard Medical School, she joined the faculty of Northwestern University where she is the Weinberg Family Distinguished Professor of Life Sciences. She is a fellow of the American Academy of Arts and Sciences and a member of the National Academy of Sciences. The Rosenzweig laboratory uses structural, biochemical, and biophysical approaches to attack problems at the forefront of bioinorganic chemistry. Their work has been honored recently by the Royal Society of Chemistry Joseph Chatt Award and the American Chemical Society Alfred Bader Award in Bioinorganic or Bioorganic Chemistry.

which offers the possibility of deployable smaller-scale methods with higher conversion efficiencies and less environmental impact.[7-9] Aerobic biological methane activation occurs in a group of methane-consuming bacteria called methanotrophs.[10,11] In contrast to energy-intensive industrial processes, methanotrophs activate methane at ambient temperature and pressure. Harnessing this unique ability could dramatically alter industrial methane processing practices.[12-14]

Aerobic methanotrophs were historically divided into two groups based on metabolic pathways, membrane lipid content, and physical characteristics. *Gammaproteobacteria* comprise the first group, commonly referred to as type I. These methanotrophs are distinguished by their use of the ribulose monophosphate (RuMP) pathway for carbon assimilation,[15,16] membranes comprising mainly 14-16 carbon phospholipids,[17] and disc-shaped intracytoplasmic membrane (ICM) structures. The second group, type II, consists of *Alphaproteobacteria* that use the serine pathway,[16] have primarily 18-carbon membrane phospholipids in their membranes,[18] and exhibit ICMs along the periphery of the cells. As new species have been characterized, types I and II have become synonymous with *Gammaproteobacteria* and *Alphaproteobacteria*.[19] A third group of methanotrophs, the *Verrucomicrobia*, was discovered recently.[20] These methanotrophs live at extreme temperatures, use the Calvin-Benson-Bassham cycle, and possess mainly saturated phospholipids.[21,22] Methanotrophs of all types are common in soils, rice paddies, swamps, and lakes where they have access to anthropogenic and bacterial sources of methane.[10] In addition, methanotrophs inhabit the tundra,[23] salt lakes,[24,25] and volcanic soil[26-29] where they oxidize methane under extreme conditions of temperatures, salinity, and acidity. Understanding the enzymes involved in methane activation under these wide-ranging conditions is critical to realizing the biotechnological potential of methanotrophs.

Methane activation is accomplished by methane monooxygenase enzymes (MMOs), which convert methane to methanol in the first step of methanotroph metabolism (eq. 1).

$$CH_4 + O_2 + 2e^- + 2H^+ \longrightarrow CH_3OH + H_2O \quad \text{(eq. 1)}$$

Methanol is then converted to formaldehyde by methanol dehydrogenase (MDH), after which the metabolic pathways diverge depending on the type of methanotroph.[16] There are two types of MMO: the copper-dependent, membrane-bound or particulate methane monooxygenase (pMMO) and the iron-dependent, soluble methane monooxygenase (sMMO).[30-32] pMMO is the primary MMO in nature and is present in all methanotrophs except a few species from the *Methylocella*[33,34] and *Methyloferula*[35] genera, which only possess sMMO.[11] pMMO is typically housed within extensive ICM structures,[36,37] and is highly abundant, representing ~20% of the total protein in the cell.[38,39] Under copper-starved conditions, some methanotrophs utilize sMMO, expression of which is regulated by a poorly-understood mechanism called the copper switch.[40,41] Once copper becomes available, sMMO expression is downregulated by 2-3 orders of magnitude, ICMs form, and pMMO is mildly upregulated.[42]

Although pMMO is more prevalent across methanotroph species, progress toward elucidating its active site and mechanism has been hampered by challenges intrinsic to handling integral membrane proteins. By contrast, sMMO, which is more amenable to study due to its soluble nature, is better understood. One challenge common to the two MMOs is the lack of a recombinant expression system.[43-46] The catalytic components of sMMO and pMMO must instead be isolated and purified directly from native methanotrophs, precluding generation of site-directed mutants. Nevertheless, each MMO has been studied extensively by biochemical, spectroscopic, and structural techniques. Several key aspects of both MMOs have been revisited in the past five years, altering and enriching our understanding of how these enzymes work. Here we review the current state of knowledge with an emphasis on recent developments and areas of controversy.

2. Particulate methane monooxygenase

2.1. Overall architecture

pMMO consists of three subunits encoded by the *pmoCAB* operon, which is present in up to three copies in the methanotroph genome, depending on the species.[27,47-55] Most methanotrophs also possess up to two extra copies of *pmoC* that are relatively divergent from those in the *pmoCAB* operons.[56,57] Since methanotrophs are frequently identified by detection of the *pmoA* gene in soil or marine bacterial populations using mRNA probes, *pmoA* genes are highly represented in databases.[58]

Crystal structures of pMMOs from five species have been determined.[59-63] The three subunits, PmoA (α), PmoB (β), and PmoC (γ), form an αβγ protomer, and three protomers related by a threefold axis of symmetry form the full $(\alpha\beta\gamma)_3$ oligomer (Fig. 1). This trimer, observed in all pMMO structures, adopts a cylindrical shape approximately 90 Å in diameter and 105 Å in length. PmoA (24 kDa) and PmoC (22 kDa) are composed of seven and five transmembrane helices, respectively, and are almost entirely embedded in the lipid bilayer. PmoB (42 kDa) comprises a soluble domain of two cupredoxin-like folds that are connected by two transmembrane helices.[59] In crystal structures of pMMO from type II methanotrophs,[60-62] an ~20 residue helix cocrystallizes with the full complex, adjacent to each PmoC subunit with a lipid mediating the interaction.[62] This helix has yet to be identified, and is reminiscent of supernumerary subunits found in the crystal structures of some respiratory complexes.[64] Additional lipids have been observed in the pMMO crystal structures, and may regulate activity and assembly.[62]

An ~25 residue region of the PmoC subunit facing the interior of the trimer is missing in every pMMO structure (Fig. 1). This sequence, corresponding to residues 200-223 in *Methylocystis* species strain (*Mc.* sp.) Rockwell pMMO,[62] is not observed in the electron density maps and therefore cannot be modeled. Importantly, these residues correspond to the most highly conserved part of the PmoC sequence[65] and contain multiple potential metal-binding residues (Fig. 2). In the case of *Methylomicrobium (Mm.) alcaliphilum* 20Z pMMO, 60% of the PmoC subunit could not be modeled.[63] The disorder may be related to destabilization and loss of pMMO activity

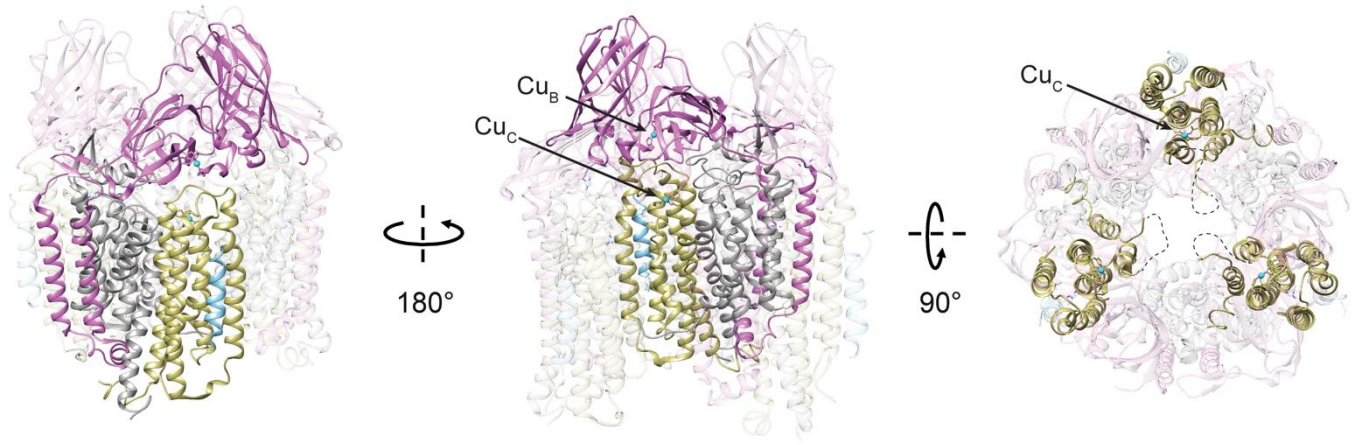

Fig. 1 Crystal structure of pMMO from *Mc.* sp. Rockwell (PDB accession code 4PI0). The PmoB subunits are shown in pink, the PmoA subunits are shown in gray, the PmoC subunits are shown in yellow, and the unidentified helix is shown in blue. Copper ions are shown as cyan spheres. In the two left images, a single αβγ protomer is highlighted. In the right top-down image, the PmoC subunits are highlighted and the location of the unmodeled, highly conserved region is marked with a dashed line.

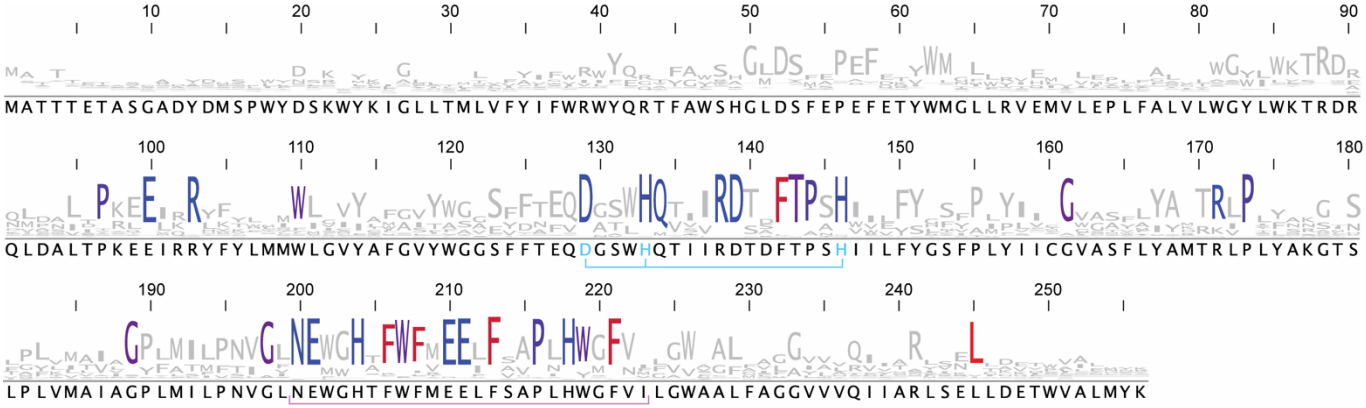

Fig. 2 Sequence conservation logo for PmoC. The logo was generated from an alignment of 451 representative sequences >170 amino acids in length from PF04896 and TIGR03078 clustered at 100% identity against a hidden Markov model constructed from 132 representative nodes clustered at 50% identity using the EFI-EST webtool.[65] Residues that are conserved in 80% of sequences or more are colored from blue to red in increasing hydrophobicity. The conserved Cu$_C$-coordinating residues are in cyan while the flexible loop is underlined in pink. The sequence is numbered using the *Mc.* sp. Rockwell PmoC numbering (Met49242_1455) and sequences were downloaded from the JGI/IMG database.

upon detergent solubilization and purification (~100-fold less than in vivo).[31,63] Activity of purified pMMO can be restored or improved by reconstitution into bicelles or nanodiscs,[63] suggesting that structural studies of pMMO in a native-like lipid environment could resolve the nature of this region.

2.2. Metal binding sites

The pMMO crystal structures reveal up to three copper binding sites per protomer. These sites are referred to as the bis-His site, the Cu$_B$ site, and the Cu$_C$ site. The residues coordinating the Cu$_B$ and Cu$_C$ sites are conserved in almost all pMMOs as well as in the homologous enzyme ammonia monooxygenase (AMO) and related hydrocarbon monooxygenases.[66-68] X-ray absorption spectroscopy (XAS), advanced paramagnetic resonance spectroscopies, and mass spectrometry have also been used extensively to probe the pMMO copper centers, with a focus on correlating spectroscopic and crystallographic data.

The bis-His site is located in the soluble region of PmoB between the two cupredoxin domains and coordinated by two histidines, His 48 and His 72 in *Methylococcus (M.) capsulatus* (Bath) pMMO. This site is only occupied in the *M. capsulatus* (Bath) pMMO structure,[59] and His 48 is replaced with asparagine in pMMOs from type II methanotrophs. Notably, the site is also devoid of metal in the *Mm. alcaliphilum* 20Z pMMO structure despite the presence of both histidine ligands.[63] It remains unclear whether the bis-His site is a crystallographic artifact or is biologically relevant, but these observations suggest that it is not essential for methane oxidation. In *M. capsulatus* (Bath) whole-cell EPR studies, a single Cu(II) signal attributable to the Cu$_B$ site is observed,[69,70] indicating that the bis-His site is either unoccupied by copper in vivo or contains Cu(I).

The Cu$_B$ site is located in the soluble region of the PmoB subunit, and is occupied by copper in all structurally characterized pMMOs.[59-63] Ligands include two histidine side chains derived from an HxH motif and the N-terminal histidine along with its amino group (His29, His 133, and His 135 in *Mc.* sp. Rockwell pMMO) (Fig. 3A). These residues are conserved in all pMMOs except those from *Verrucomicrobia*, in which the equivalent residues are methionine, proline, and glycine, which are unlikely to bind metal.[20,47,71] The Cu$_B$ site has been suggested to be analogous to the histidine brace copper active site of lytic polysaccharide monooxygenases (LPMOs) (Fig. 3B). However, there are several important differences. First, Cu$_B$ has an additional histidine ligand, of which the coordinating nitrogen occupies the axial bonding position that is open in LPMO.[72,73] Second, the non-amino-terminal histidine ligand in LPMOs coordinates

copper with its ε nitrogen atom whereas all the histidines in Cu_B use their δ nitrogen atoms. Third, the LPMO site has a tyrosine side chain oxygen within 2.6 Å of the copper ion while the shortest tyrosine-to-Cu_B distance is 5 Å (Fig. 3). Finally, the coordinating amino group is well ordered in the LPMO structures,[72] but may adopt fluctuating orientations in the Cu_B site as evidenced by poor electron density in every structure.

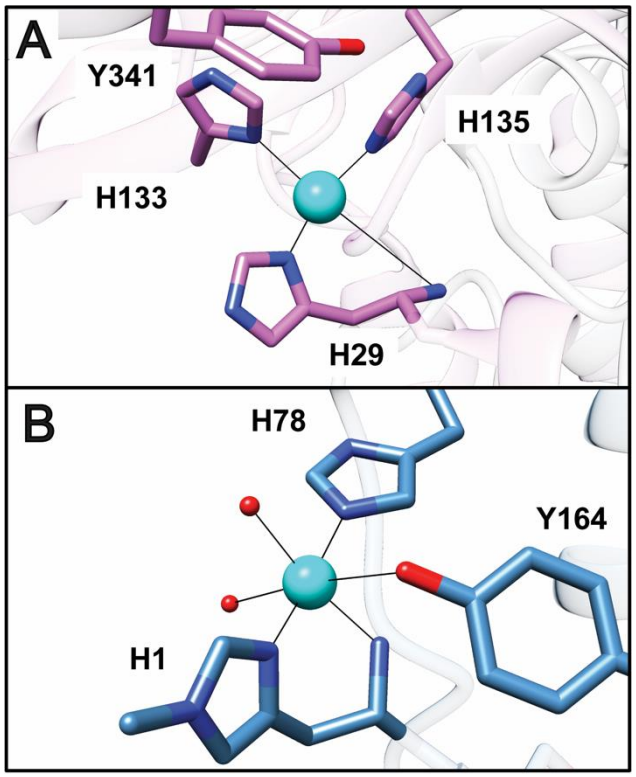

Fig. 3 Comparison of the pMMO Cu_B site to the active site of LPMO. (A) The *Mc.* sp. Rockwell pMMO Cu_B site (PDB accession code 4PI0). The shortest distance from Tyr341 to the copper ion is 5 Å. (B) The *Lentinus similis* LPMO copper active site (PDB accession code 5ACG). Solvent ligands are shown as red spheres. Methylation of the amino-terminal histidine is not a universal feature of LPMO active sites.

The nuclearity of the Cu_B site has been discussed for more than a decade. In the original crystal structure of pMMO from *M. capsulatus* (Bath), it could be modeled with either one or two copper ions, sparking the debate over its nuclearity.[59] The dinuclear model was inspired by extended X-ray absorption fine structure (EXAFS) data indicating the presence of a 2.5-2.6 Å Cu-Cu scattering interaction.[74,75] However, a computational study using quantum methods to further refine the original structure indicated that monocopper is favored at this site,[76] consistent with later and higher quality crystal structures also showing a mononuclear Cu_B site.[61-63]

Additional strong support for this model comes from a recent electron paramagnetic resonance (EPR) study of *M. capsulatus* (Bath) whole cells.[70] A single signal was observed for $^{15}N/^{63}Cu$ labeled cells with ^{15}N hyperfine splitting indicative of four equatorial nitrogen ligands. These ligands were assigned by electron nuclear double resonance (ENDOR) measurements to three histidyl imidazole side chains, a ligand assemblage only possible in the Cu_B site. Thus, not only is Cu_B mononuclear, but these data confirm that the structures recapitulate pMMO in the cell and are biologically relevant. The EPR data indicate that Cu_B is unchanged upon purification, and ^{17}O ENDOR of samples incubated with $H_2{}^{17}O$ revealed the presence of an axial $H_x{}^{17}O$ ligand not resolved in the crystal structures, of which the highest resolution is 2.68 Å.[62] The Cu_B site is therefore best described as a mononuclear Cu(II) site with square pyramidal geometry. These results are corroborated by recent native top-down mass spectrometric (nTDMS) analysis of purified pMMO reconstituted into nanodiscs, which clearly showed the presence of a single copper ion in PmoB.[77] Nevertheless, the source of the EXAFS Fourier transform feature that was fit as a Cu-Cu interaction remains unclear and must be reinvestigated in order to fully reconcile all the data.

The Cu_C site, which is conserved in all pMMOs, is located within the transmembrane domain of the PmoC subunit and includes two histidines and an aspartic acid as ligands (Asp 129, His 133, and His 146 in *Mc.* sp. Rockwell pMMO[62]) (Fig. 4). If pMMO is crystallized in zinc-containing buffer or if zinc is soaked into the crystals, zinc is present in this site.[59,61,62] In the absence of zinc, the site is occupied by copper,[60,62] and the occupancy can be increased by soaking in extra copper.[62] An EPR signal observed in purified pMMO samples has been assigned to the Cu_C site on the basis of Cu-Cu distances obtained from double electron-electron resonance (DEER) measurements.[70] The signal is not observed in whole cells, presumably because the Cu_C site is Cu(I) in vivo. Since the EPR signal assigned to the Cu_C site overlaps with that of the Cu_B site, its coordination environment is less readily determined. However, ^{15}N ENDOR is consistent with histidine ligation and ^{1}H and ^{17}O ENDOR indicate the presence of a solvent ligand.[70] nTDMS analysis of pMMO in nanodiscs also indicates binding of a single copper ion to the PmoC subunit, and copper supplementation during nanodisc formation increases the copper occupancy of PmoC.[77] Fragmentation data localizing the bound copper ion to the crystallographically-observed Cu_C site could not be obtained, however.

While the advanced paramagnetic resonance analysis is consistent with the crystallographic model for the Cu_C site, the coordination is not a foregone conclusion. The site directly abuts the unmodeled, highly conserved region of the PmoC subunit (Figs. 1, 4),[59-62] and is not even visible in the *Mm. alcaliphilum* 20Z pMMO structure.[63] Weak density suggestive of a fourth ligand has been modeled as a water molecule in the *Mc.* sp. strain M[61] and *Mc.* sp.

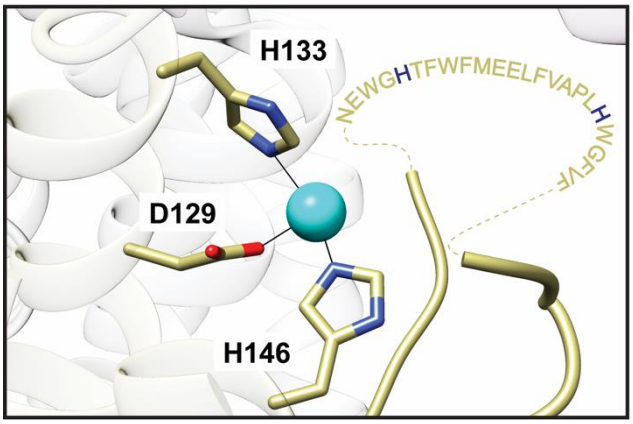

Fig. 4 The *Mc.* sp. Rockwell pMMO Cu_C site (PDB accession code 4PI0). The unmodeled highly conserved region spanning residues 200-223 is shown as amino acid one-letter codes connected to the model by dashed lines. Potential metal binding residues include two strictly conserved histidines highlighted in blue.

Rockwell pMMO structures, while soaking *Mc.* sp. Rockwell pMMO crystals in zinc led to ordering of 10 additional residues and modeling of a glutamic acid ligand not observed in the structures with copper.[62] Given the striking conservation of this region and the presence of potential metal-binding residues, it is imperative to determine its structure. It remains possible that the Cu_C EPR signal derives from a copper site that has not yet been structurally unveiled.

2.3. Identity of the active site

The location and molecular details of the pMMO active site represent one of the most important outstanding questions in biological methane activation. Methane oxidation assays using samples of pMMO demetallated and inactivated by cyanide treatment indicate that 2-3 copper ions are required for activity. Addition of excess copper inhibits activity, albeit in a reversible fashion.[46,62] While a diiron center was once proposed to be the pMMO active site,[39] there is no iron in the structures and only copper has been linked to activity. Of the crystallographically-observed copper sites, the bis-His site has been discounted because the coordinating residues are not conserved and the site is only occupied in one crystal structure.[59]

Instead, the Cu_B site has been the focus of most discussion. Computational studies have suggested that both a dinuclear[78-80] and a mononuclear[76] copper site at this location would be capable of methane oxidation. The possibility of a Cu_B active site was investigated using recombinantly expressed proteins that contain the two PmoB cupredoxin domains, form a Cu_B site similar to that in native pMMO by EPR,[70] and convert methane to methanol.[46,70] However, extensive evaluation of these proteins revealed that the methanol is not produced by their Cu_B-like site, and likely involves adventitious chemistry from the reduction of dioxygen by duroquinol, which is used as a reductant in pMMO activity assays.[70] As such, the basis for recently reported enzymatic activity of pMMO mimetics utilizing the PmoB soluble domains tethered to apo ferritin[81] is unclear. The argument for a Cu_B active site is further diminished by the replacement of the three Cu_B-coordinating histidines in the verrucomicrobial PmoB sequences with methionine, proline, and glycine.[29,47,48]

In the absence of evidence for Cu_B being the site of methane activation, attention has turned toward the Cu_C site. Two recent experimental findings are consistent with a Cu_C active site. First, nitrite, a known inhibitor of methane oxidation,[82,83] perturbs the Cu_C EPR signal, and ^{15}N ENDOR upon the addition of ^{15}N-nitrite is consistent with NO_2^- binding to Cu(II) via the oxygen atom(s).[70] Second, an increase in the copper occupancy of PmoC detected by nTDMS was correlated with increased pMMO activity.[77] These combined data suggest that copper in PmoC, regardless of whether it is located at the crystallographic Cu_C site, is the site of methane oxidation. In support of this model, mutation of the Cu_C site in a homologous hydrocarbon monooxygenase completely abrogated activity whereas mutation of the Cu_B site reduced activity, but maintained affinity for alkane substrate.[67,84] Thus, Cu_B may still play a functional or stabilizing role, accounting for the requirement of more than one copper ion for activity.[46,62] Importantly, the Cu_C ligands along with the neighboring disordered region of PmoC are conserved in all pMMOs, including those from *Verrucomicrobia*.[29,47,48] This observation underscores the potential importance of the Cu_C site, but characterization of the verrucomicrobial pMMOs, which lack the Cu_B site ligands, is imperative. *Verrucomicrobia* grow at high temperatures and low pH, conditions that may affect the structure and metal binding properties of pMMO.

2.4. Protein partners

Another unresolved issue regarding pMMO is the potential existence of larger protein complexes containing pMMO or transient protein-protein interactions between pMMO and partners. Whereas catalysis by sMMO requires interaction of the hydroxylase component (MMOH) with a reductase (MMOR) and a regulatory protein (MMOB) (vide infra),[32] pMMO activity can be obtained in vitro by addition of the reductants NADH and duroquinol to membrane-bound and detergent-solubilized samples, respectively.[85,86] Duroquinol is believed to mimic a native quinol present in the membranes, presumably ubiquinol, which directly reduces pMMO. NADH is thought to reduce the native quinol via a type 2 NADH:quinone oxidoreductase (NDH-2) that has been observed to copurify with pMMO,[38,87,88] although there is no evidence for direct interactions between pMMO and NDH-2. Reduction of pMMO by quinols using this pathway has been referred to as the "redox-arm mode" of electron delivery.[89]

Electron delivery to pMMO has also been proposed to occur via methanol oxidation to formaldehyde by MDH.[90] In this "direct coupling mode," electrons are funneled to pMMO through the cytochrome *c* electron acceptor of MDH. Support for both the redox arm and direct coupling models as well as a combination thereof, "uphill electron transfer," has been obtained from genome-wide metabolic modeling for several methanotrophs.[89,91-95] Direct coupling would be facilitated by complexation with MDH, allowing direct transfer of methanol from pMMO to the MDH active site, and a pMMO-MDH complex has been proposed on the basis of low resolution cryoelectron microscopy studies.[96] While this complex has not been isolated biochemically, transient interactions between several pMMOs and their cognate MDHs have been detected.[97,98] How the MDH dimer (Fig. 5A) interacts with the pMMO trimer is not clear. Resolving the nature of pMMO's interaction with electron donor proteins is an important goal for future studies.

Finally, the loss of pMMO activity upon solubilization and purification may be due in part to separation from other protein components necessary for stabilization, copper loading, and delivery of electrons and/or protons. Recent work has suggested that the PmoD protein, found exclusively in methane- and ammonia-oxidizing bacteria and sometimes encoded within the same operon as the pMMO subunits, is one such component.[99] Genetic disruption experiments in *Methylosinus* (*Ms.*) *trichosporium* OB3b indicate that PmoD is important for growth under pMMO-utilizing conditions. PmoD consists of a cupredoxin-like periplasmic domain (Fig. 5B) followed by a C-terminal transmembrane helix. In isolation, the

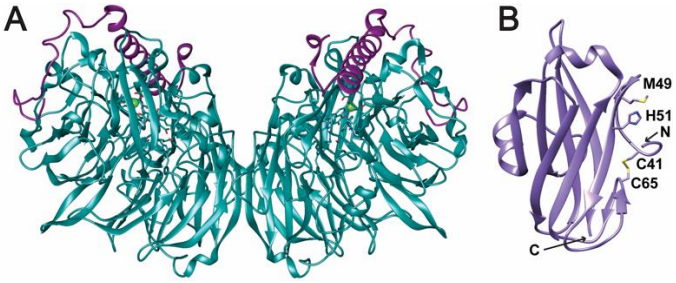

Fig. 5 Potential protein interaction partners of pMMO. (A) *M. capsulatus* (Bath) MDH (PDB accession code 4TQO). The α subunits are shown in teal and the β subunits are shown in violet. The pyrroloquinoline quinone (PQQ)/calcium ion cofactor is shown as sticks and a green sphere. (B) The periplasmic domain of PmoD from *Mc.* sp. Rockwell (PDB accession code 6CPD). Conserved residues involved in formation of a Cu_A-like site between two monomers are highlighted. In this structure, the two conserved cysteines form a disulfide bond. A predicted transmembrane helix at the C-terminus is not present in this structure.

periplasmic domain forms an unusual Cu_A-like site with a symmetric ligand set derived from a PmoD homodimer; this form of the protein has not been crystallographically characterized.[100] It remains unclear whether this site forms in vivo in the presence of the transmembrane domain. Direct interactions between PmoD and pMMO have not been established, but the role of this protein in biological methane activation warrants further study.

3. Soluble methane monooxygenase

3.1. Overall architecture

While most methanotrophs rely solely on pMMO for methane oxidation, some have the ability to express sMMO under copper-starvation conditions.[11,37,40] sMMO consists of multiple proteins encoded within the *mmoXYBZDC* operon.[101] The *mmoX, mmoY, and mmoZ* genes encode the α, β, and γ subunits of the hydroxylase component (MMOH), which houses a nonheme diiron active site. The *mmoB* gene encodes the regulatory protein, MMOB, and *mmoC* encodes the reductase, MMOR, which reduces the diiron site via NADH and contains FAD and a [2Fe-2S] cluster as cofactors. MMOB increases the reaction rate of MMOH with dioxygen by 1000-fold.[102,103] MMOD is not necessary for sMMO function and instead has an inhibitory effect on activity.[104,105] Like pMMO, MMOH must be isolated from the native organism for biochemical studies, but MMOB, MMOR, and MMOD can be expressed in *E. coli*.

sMMO systems from *M. capsulatus* (Bath) and *Ms. trichosporium* OB3b have been structurally characterized. MMOH is a dimer comprising the three subunits in an $(\alpha\beta\gamma)_2$ arrangement (Fig. 6A).[106,107] The diiron active site, housed within a four-helix bundle, is coordinated by two histidine and four carboxylate ligands from the α subunit (Glu 114, His 147 to Fe1, Glu 209, Glu 243, His 246 to Fe2, Glu 144 bridging). In the resting Fe(III)Fe(III) state, the iron ions are bridged by two hydroxo groups (Fig. 7A). Upon reduction to the Fe(II)Fe(II) state, Glu 243 displaces a bridging hydroxo group, bridging the two irons, while coordinating Fe2 in a bidentate fashion (Fig. 7B).[108,109] A number of MMOH structures have been determined in the presence of hydrocarbon substrate and product analogs, xenon gas, and different metal ions.[31] The MMOB and MMOC structures have been determined by NMR, with the [2Fe-2S] and FAD/NADH domains of MMOC characterized separately.[110-113]

In addition, crystal structures of MMOH in complex with MMOB[109,114] and in complex with MMOD[115] have been reported. Both MMOB and MMOD bind symmetrically to MMOH, with one molecule interacting with each αβγ protomer (Figs. 6B,C). Upon binding to MMOH, primarily to the α subunit, MMOB's flexible N-terminal tail of ~35 residues forms a ring-like structure on the MMOH surface. The C-terminal region of MMOB becomes ordered as well. Several MMOH helices are reorganized, and the resultant side chain rearrangements directly affect the active site.[109,114] In the initial *M. capsulatus* (Bath) MMOH-MMOB structure, Glu 243 shifts to its reduced conformation,[114] but this change is not observed in a recent X-ray free electron laser (XFEL) structure of *Ms. trichosporium* MMOH-MMOB determined at room temperature, suggesting that photoreduction, rather than MMOB binding, caused the shift.[109] The binding site for MMOD, as observed in the *Ms. sporium* strain 5 MMOH-MMOD complex structure, overlaps with that of MMOB. MMOD disrupts the N-terminus of the β subunit, which wraps around the α subunit in each protomer, and affects Fe1, causing dissociation of His 147 and a shift of Glu 114 to bidentate.[115]

There is no structure of the MMOH-MMOR complex, but the MMOR binding site mapped by hydrogen-deuterium exchange, chemical crosslinking, and computational docking[116-119] overlaps with that of MMOB. Overlapping sites are consistent with inhibition of MMOR binding by MMOB,[114,120] and suggest a model in which MMOR and MMOB compete for binding to MMOH, although an

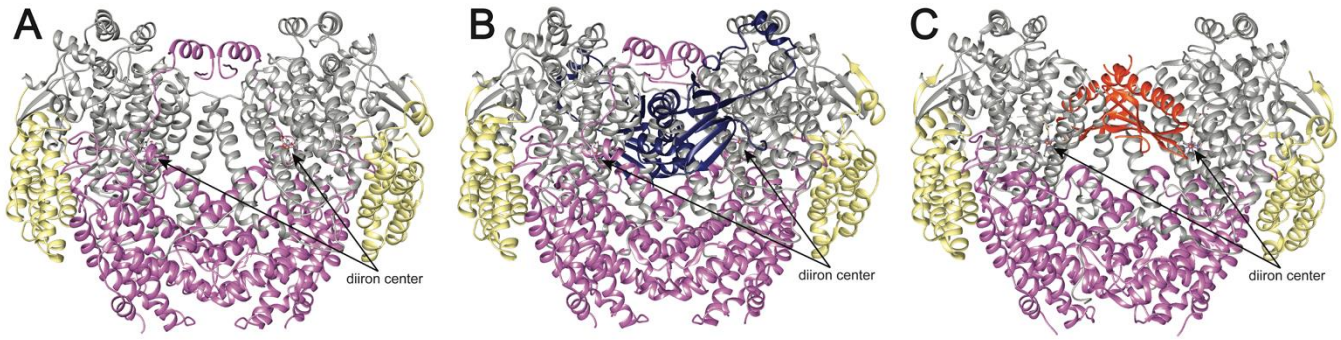

Fig. 6 Structures of sMMO. (A) *M. capsulatus* (Bath) MMOH (PDB accession code 1MTY). The α subunits are shown in gray, the β subunits are shown in pink, and the γ subunits are shown in yellow. The iron ions are shown as orange spheres with the ligands shown as sticks. (B) *M. capsulatus* (Bath) MMOH-MMOB complex (PDB accession code 4GAM). MMOB is shown in dark blue. (C) *M. sporium* strain 5 MMOH-MMOD complex (PDB accession code 6D7K). MMOD is shown in orange.

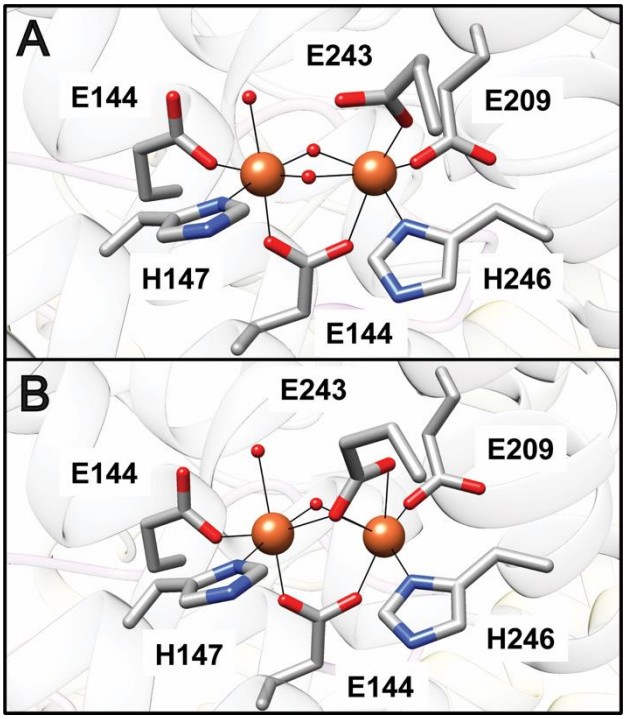

Fig. 7 The sMMO active site. (A) The Fe(III)Fe(III) site in *M. capsulatus* (Bath) $MMOH_{ox}$ (PDB accession code 1MTY). (B) The Fe(II)Fe(II) site in *M. capsulatus* (Bath) $MMOH_{red}$ (PDB accession code 1FYZ). Iron ions are shown as orange spheres and solvent ligands are shown as red spheres.

MMOH-MMOB-MMOR ternary complex has been detected.[118] In this model, MMOR binds first and reduces the diiron site, which causes MMOR to lose affinity for MMOH and be replaced by MMOB. Reduced MMOH ($MMOH_{red}$) has higher affinity for MMOB and binding of MMOB allows formation of reactive intermediates and substrate oxidation. MMOB is then released followed by product egress from the active site. It is possible that MMOB dissociates entirely or remains tethered with its N-terminal ring region to allow the cycle to begin again with MMOR binding.[116] However, this model is not compatible with the observation that MMOB decreases the redox potential of MMOH,[121,122] necessitating that it bind oxidized MMOH ($MMOH_{ox}$) with a higher affinity than $MMOH_{red}$. In addition, fluorescence titrations using labeled MMOB indicate a higher affinity for $MMOH_{ox}$ than MMO_{red}.[123] These discrepancies have been suggested to derive from hysteretic effects on the redox potential.[32]

3.2. Pores and cavities

While the most intense discussions surrounding pMMO structure have focused on the metal centers and their possible roles in catalysis, the diiron active site of sMMO has been well established for >30 years.[124,125] Ongoing debate has instead focused on substrate specificity and access to the active site and the role of MMOB therein. Access to the active site has been considered in the context of three distinct cavities observed in the MMOH crystal structures. The first cavity contains the diiron active site, is ~12 Å from the bulk solvent, and is connected via a pore to the surface of the enzyme. This pore is gated by residues Thr 213, Asn 214, and Glu 240.[126] The second cavity is adjacent to the first, but is blocked by residues Phe 188 and Leu 110 in structures of MMOH alone. This cavity is connected to a third large cavity, and all three cavities have been shown to bind halogenated alkanes and xenon gas, suggesting that they form routes for methane, dioxygen, and product access.[127,128]

Crystal structures of MMOH-MMOB revealed shifts in residues gating the pore and cavities. Upon MMOB binding, new interactions involving MMOH residues Ser 111, Asn 214, Thr 213, and Glu 240 close the pore. In the original *M. capsulatus* (Bath) MMOH-MMOB structure, shifts in residues Phe 188 and Leu 110 connect the first and second cavities, and were proposed to allow methane and dioxygen to access the reduced diiron site.[114] However, kinetic data are not consistent with methane traversing 35-40 Å in cavities prior to reaction at the active site.[129 32,130] Moreover, in recent high resolution structures of the *Ms. trichosporium* OB3b MMOH-MMOB complex, the shift in Phe 188 is only observed upon binding of bulky substrates. The cavities remain separated in $MMOH_{red}$ as well as in the XFEL structures of $MMOH_{ox}$-MMOB and $MMOH_{red}$-MMOB, suggesting that MMOB may actually serve to close, rather than open, this bottleneck.[131] An alternative path, designated the W308-tunnel, has been detected using a probe with solvent radius 1.1 Å instead of the previously used water solvent radius of 1.4 Å. This tunnel, gated by Trp 308 and Pro 215 (Fig. 8), is lined with highly conserved hydrophobic residues, and is open in the $MMOH_{red}$-MMOB structure. The use of this narrow tunnel is more consistent with the accumulated kinetic data, and variants of MMOB designed to block this tunnel significantly affect the rate of diiron active site oxidation, supporting its role in dioxygen access.[131]

3.3. Dioxygen and methane activation

In contrast to pMMO, the mechanisms of dioxygen and methane activation by sMMO have been studied in detail. The catalytic cycle of MMOH in the presence of MMOB has been probed extensively by single-turnover kinetics and spectroscopy using chemical reductants, and has been recently reviewed elsewhere.[32,132] In brief, reaction of $MMOH_{red}$ with dioxygen yields intermediate O,[102,103,133] an Fe(II)Fe(II) species that converts sequentially to intermediates P*, P, and

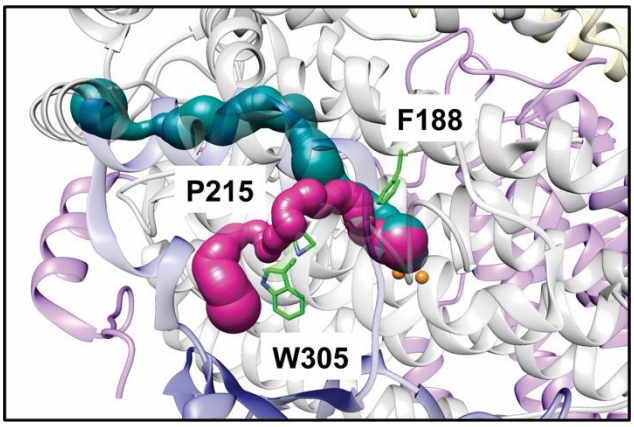

Fig. 8 Cavities and tunnels in the *Ms. trich*osporium OB3b $MMOH_{red}$-MMOB XFEL structure (PDB accession code 6YDI). The α subunits are shown in gray, the β subunits are shown in pink, the γ subunits are shown in yellow, and MMOB is shown in dark blue. The W308 tunnel is shown in magenta and the previously identified chain of cavities is shown in teal. Key gating residues are highlighted in green sticks.

Q.[102,134-136] Intermediate P* is also an Fe(II)Fe(II) species,[136] while P is an Fe(III)Fe(III) peroxo species,[134,135] the exact structure of which remains unclear.[32] As the species that reacts with methane, intermediate Q has been the subject of much discussion. Two antiferromagnetically coupled high-spin Fe(IV) ions are present,[137-139] but the geometry remains under debate, with evidence supporting both diamond and open core geometries.[139-143] Once Q reacts with methane, intermediate T is formed, followed by methanol release and return to $MMOH_{ox}$.[139]

The mechanism of methane activation by Q has also been investigated extensively, both computationally[144,145] and experimentally. Experimental approaches have leveraged sMMO's wide substrate range (cyclic hydrocarbons and cubanes, linear alkanes C1-C8)[146-148] to assess reactions with chiral[149,150] and radical clock[151-154] substrates, which provide insight into the possible existence of radical intermediates. These studies are consistent with a hydrogen abstraction mechanism,[32] but are complicated by the use of nonnatural substrates. Notably, studies using deuterated methane revealed a remarkable kinetic isotope effect (KIE) of 50, which is not observed with other substrates[155,156] and is suggestive of hydrogen tunneling. Conformational changes upon MMOB binding have been proposed to selectively guide methane to the active site in such a way as to optimize tunneling.[32]

4. Protein engineering

Many of the unresolved questions surrounding both MMOs could be addressed by site-directed mutagenesis. For pMMO, mutation of the residues coordinating the crystallographically-observed metal centers would go a long way toward establishing functional relevance as would alteration of the highly conserved part of PmoC that is not observed crystallographically. Substrate specificity and mechanistic studies would also be facilitated. For sMMO, the ability to heterologously generate MMOB variants has helped detect intermediates[129] and has provided insight into control of substrate access to intermediate Q,[129,130,156] but the roles of the different cavities and channels can only be probed in a systematic fashion by using MMOH variants. Moreover, commercially viable biological methane activation may require engineering of either MMO to have increased methane oxidation rates,[8] which would be more feasible in a heterologous expression system.

However, attempts at heterologous expression of MMOH or pMMO have been largely unsuccessful. Recombinant versions of the PmoB subunit recapitulate some of the spectroscopic properties of pMMO, but are unstable in the absence of fusion proteins and are not catalytically active.[46,70] The N-terminal cupredoxin domain of the homologous AmoB subunit from *Nitrosocaldus yellowstonii*, which lacks the C-terminal cupredoxin domain, has been recombinantly expressed and crystallographically characterized, but does not exhibit methane oxidation activity.[68] Expression of intact pMMO has been reported in *Rhodococcus erythropolis* LSSE8-1, albeit with whole cell activity 340 times less than that of *Ms. trichosporium* OB3b.[8,45] Besides likely issues involving insertion of the pMMO subunits into the membrane and proper trimer assembly, an obstacle specific to expression of functional pMMO may be the lack of ICMs in heterologous hosts. In most methanotrophs, pMMO is localized to these intracellular structures,[17,37,40,157] which could play a role in structuring the enzyme or concentrating methane.[8] The presence of ICMs and the location of pMMO in the verrucomicrobial methanotrophs remain unclear, however.[22]

While enzymes related to MMOH such as toluene and phenol hydroxylases have been expressed in *E. coli*,[158,159] the only reported heterologous expression of MMOH is in *Pseudomonas,* although methane oxidation by these strains has not been reported.[43] Neither this system nor the pMMO *Rhodococcus erythropolis* LSSE8-1 expression system[45] resulted in the ability to generate variants or isolate recombinant MMOs for further study. As an alternative approach, *Ms. trichosporium* OB3b MMOH genes with mutations of interest have been reintroduced into a *Ms. trichosporium* OB3b strain with the *smmo* operon partially deleted. This strain can be grown using pMMO, with expression of the variant MMOHs occurring as copper levels decline.[160,161] Several variants have been studied using this method, primarily focusing on residues in the α subunit surrounding the diiron center.[161-163] However, this system requires optimization to be practical for generation of large numbers of variants for protein purification and characterization.

An analogous strategy for pMMO is more complicated because most methanotroph genomes contains multiple copies of the *pmo* operon. Genetic tools have been developed for the methanotroph *Methylotuvimicrobium buryatense* 5GB1C (formerly *Methylomicrobium buryatense* 5GB1C[164]),[165,166] which has been used for metabolic engineering[16] and only contains one copy of the pMMO genes. In principle, it should be possible to obtain point mutants of pMMO using these tools and growing under sMMO-producing conditions to mitigate any growth defects from an impaired pMMO. However, such attempts have not been successful, perhaps because for unknown reasons, pMMO remains important for cell growth under sMMO-producing conditions. This notion is consistent with the observation that pMMO is still expressed under conditions of copper starvation and only mildly upregulated when copper is available.[42] CRISPR-Cas9, which has been developed for methanotrophs, presents another potential route to variants, but the current method has very low editing efficiency and has not yet been demonstrated to be effective for this purpose.[167]

Conclusions

The unique lifestyle of methanotrophs presents intriguing possibilities for methane utilization and bioremediation. Their wide variety of habitats highlights the effectiveness of the MMO-based carbon assimilation strategy. For pMMO, progress has been made in understanding the nuclearity of the Cu_B site and the importance of the Cu_C site. Further studies of pMMO in a lipid environment and of the verrucomicrobial pMMOs promise to shed light on the active site location and structure, bringing the field closer to determining the reaction mechanism. Beyond the pMMO trimer itself, the possibilities of PmoD and MDH as interaction partners represent an important future direction. For sMMO, new structures of MMOH

complexes, some determined using an XFEL, have revealed in detail the effects of MMOB and MMOD on MMOH structure and have delineated new pathways for substrate access to the diiron active site. The geometry of intermediate Q, the relative importance of different cavities in the MMOH structures, and the sequence of events involving MMOB and MMOR binding require additional studies. Studies of both MMOs await development of effective heterologous expression systems, which could be used to generate variants and as a platform for protein engineering. The combination of detailed chemical understanding and protein engineering could finally realize the potential of methanotrophs to add value[14] and even help save the planet.

Conflicts of interest

There are no conflicts to declare.

Acknowledgements

The pMMO and PmoD projects in the Rosenzweig laboratory are supported by National Institutes of Health Grant R35 GM118035 and United States Department of Energy Grant DE-SC0016284, respectively.

References

1 S. E. M. Fletcher and H. Schaefer, *Science*, 2019, **364**, 932-933.
2 M. Saunois, R. B. Jackson, P. Bosquet, B. Poulter and J. G. Canadell, *Environ. Res. Lett.*, 2016, **11**, 120207.
3 G. Myhre, D. Shindell, F.-M. Bréon, W. Collins, J. Fuglestvedt, J. Huang, D. Koch, J.-F. Lamarque, D. Lee, B. Mendoza, T. Nakajima, A. Robock, G. Stephens, T. Takemura and H. Zhang, in *Climate Change 2013: The Physical Science Basis. Contribution of Working Group I to the Fifth Assessment Report of the Intergovernmental Panel on Climate Change*, ed. T. F. Stocker, D. Qin, G.-K. Plattner, M. Tignor, S.K. Allen, J. Boschung, A. Nauels, Y. Xia, V. Bex and P.M. Midgley Cambridge University Press, 2013.
4 C. A. Haynes and R. Gonzalez, *Nat. Chem. Biol.*, 2014, **10**, 331-339.
5 S. J. Blanksby and G. B. Ellison, *Acc Chem Res*, 2003, **36**, 255-263.
6 D. A. Wood, C. Nwaoha and B. F. Towler, *J. Nat. Gas Sci. Eng.*, 2012, **9**, 196-208.
7 X. M. Ge, L. C. Yang, J. P. Sheets, Z. T. Yu and Y. B. Li, *Biotech. Adv.*, 2014, **32**, 1460-1475.
8 T. J. Lawton and A. C. Rosenzweig, *Curr. Opin. Chem. Biol.*, 2016, **35**, 142-149.
9 J. M. Clomburg, A. M. Crumbley and R. Gonzalez, *Science*, 2017, **355**.
10 R. S. Hanson and T. E. Hanson, *Microbiol. Rev.*, 1996, **60**, 439-471.
11 J. D. Semrau, A. A. Dispirito and S. Yoon, *FEMS Microbiol. Lett.*, 2010, **34**, 496-531.
12 M. Kwon, A. Ho and S. Yoon, *Appl. Microbiol. Biotechnol.*, 2019, **103**, 1-8.
13 C. A. Henard, T. G. Franklin, B. Youhenna, S. But, D. Alexander, M. G. Kalyuzhnaya and M. T. Guarnieri, *Front. Microbiol.*, 2018, **9**, 2610.
14 P. J. Strong, S. Xie and W. P. Clarke, *Environ. Sci. Technol.*, 2015, **49**, 4001-4018.
15 J. P. Bowman, L. I. Sly and E. Stackebrandt, *Int. J. Syst. Bacteriol.*, 1995, **45**, 182-185.
16 M. G. Kalyuzhnaya, A. W. Puri and M. E. Lidstrom, *Metab. Eng.*, 2015, **29**, 142-152.
17 S. L. Davies and R. Whittenbury, *J. Gen. Microbiol.*, 1970, **61**, 227-232.
18 R. A. Makula, *J. Bacteriol.*, 1978, **134**, 771-777.
19 C. Knief, *Front. Microbiol.*, 2015, **6**, 1346.
20 H. J. M. Op den Camp, T. Islam, M. B. Stott, H. R. Harhangi, A. Hynes, S. Schouten, M. S. M. Jetten, N.-K. Birkeland, A. Pol and P. F. Dunfield, *Environ. Microbiol. Rep.*, 2009, **1**, 293-306.
21 A. F. Khadem, A. Pol, A. Wieczorek, S. S. Mohammadi, K. J. Francoijs, H. G. Stunnenberg, M. S. Jetten and H. J. M. Op den Camp, *J. Bacteriol.*, 2011, **193**, 4438-4446.
22 M. C. van Teeseling, A. Pol, H. R. Harhangi, S. van der Zwart, M. S. Jetten, H. J. M. Op den Camp and L. van Niftrik, *Appl. Environ. Microbiol.*, 2014, **80**, 6782-6791.
23 J. P. Bowman, S. A. McCammon and J. H. Skerratt, *Microbiology*, 1997, **143**, 1451-1459.
24 M. G. Kalyuzhnaya, V. N. Kmelenina, N. G. Starostina, S. B. Baranova, N. E. Suzina and Y. A. Trotsenko, *Mikrobiologiia*, 1998, **67**, 438-444.
25 V. N. Khmelenina, M. G. Kalyuzhnaya, N. G. Starostina, N. E. Suzina and Y. A. Trotsenko, *Curr. Microbiol.*, 1997, **35**, 257-261.
26 A. Pol, K. Heijmans, H. R. Harhangi, D. Tedesco, M. S. M. Jetten and H. J. M. Op den Camp, *Nature*, 2007, **450**, 874-878.
27 S. B. Hou, K. S. Makarova, J. H. W. Saw, P. Senin, B. V. Ly, Z. M. Zhou, Y. Ren, J. M. Wang, M. Y. Galperin, M. V. Omelchenko, Y. I. Wolf, N. Yutin, E. V. Koonin, M. B. Stott, B. W. Mountain, M. A. Crowe, A. V. Smirnova, P. F. Dunfield, L. Feng, L. Wang and M. Alam, *Biol. Direct*, 2008, **3**, 26.
28 P. F. Dunfield, A. Yuryev, P. Senin, A. V. Smirnova, M. B. Stott, S. Hou, B. Ly, J. H. Saw, Z. Zhou, Y. Ren, J. Wang, B. W. Mountain, M. A. Crowe, T. M. Weatherby, P. L. E. Bodelier, W. Liesack, L. Feng, L. Wang and M. Alam, *Nature*, 2007, **450**, 879-882.
29 T. Islam, S. Jensen, L. J. Reigstad, O. Larsen and N. K. Birkeland, *Proc. Natl. Acad. Sci. USA*, 2008, **105**, 300-304.
30 M. O. Ross and A. C. Rosenzweig, *J. Biol. Inorg. Chem.*, 2017, **22**, 307-319.
31 S. Sirajuddin and A. C. Rosenzweig, *Biochemistry*, 2015, **54**, 2283-2294.
32 R. Banerjee, J. C. Jones and J. D. Lipscomb, *Annu. Rev. Biochem.*, 2019, **88**, 409-431.
33 P. F. Dunfield, V. N. Khmelenina, N. E. Suzina, Y. A. Trotsenko and S. N. Dedysh, *Int. J. Syst. Evol. Microbiol.*, 2003, **53**, 1231-1239.
34 S. N. Dedysh, C. Knief and P. F. Dunfield, *J. Bacteriol.*, 2005, **187**, 4665-4670.
35 A. V. Vorobev, M. Baani, N. V. Doronina, A. L. Brady, W. Liesack, P. F. Dunfield and S. N. Dedysh, *Int. J. Syst. Evol. Microbiol.*, 2011, **61**, 2456-2463.
36 R. Whittenbury, K. C. Phillips and J. F. Wilkinson, *J. Gen. Microbiol.*, 1970, **61**, 205-218.
37 S. D. Prior and H. Dalton, *J. Gen. Microbiol.*, 1985, **131**, 155-163.
38 D. W. Choi, R. C. Kunz, E. S. Boyd, J. D. Semrau, W. E. Antholine, J. I. Han, J. A. Zahn, J. M. Boyd, A. M. de la Mora and A. A. DiSpirito, *J. Bacteriol.*, 2003, **185**, 5755-5764.
39 M. Martinho, D. W. Choi, A. A. DiSpirito, W. E. Antholine, J. D. Semrau and E. Münck, *J. Am. Chem. Soc.*, 2007, **129**, 15783-15785.

40 S. H. Stanley, S. D. Prior, D. J. Leak and H. Dalton, *Biotechnol. Lett.*, 1983, **5**, 487-492.
41 A. K. Nielsen, K. Gerdes and J. C. Murrell, *Mol. Microbiol.*, 1997, **25**, 399-409.
42 G. E. Kenney, M. Sadek and A. C. Rosenzweig, *Metallomics*, 2016, **8**, 931-940.
43 D. Jahng and T. K. Wood, *Appl. Environ. Microbiol.*, 1994, **60**, 2473-2482.
44 J. C. Murrell, B. Gilbert and I. R. McDonald, *Arch. Microbiol.*, 2000, **173**, 325-332.
45 Z. Gou, X.-H. Xing, M. Luo, H. Jiang, B. Han, H. Wu, L. Wang and F. Zhang, *FEMS Microbiol. Lett.*, 2006, **263**, 136-141.
46 R. Balasubramanian, S. M. Smith, S. Rawat, T. L. Stemmler and A. C. Rosenzweig, *Nature*, 2010, **465**, 115-119.
47 T. Kruse, C. M. Ratnadevi, H. A. Erikstad and N. K. Birkeland, *BMC Genomics*, 2019, **20**, 642.
48 S. Y. Anvar, J. Frank, A. Pol, A. Schmitz, K. Kraaijeveld, J. T. den Dunnen and H. J. Op den Camp, *BMC Genomics*, 2014, **15**, 914.
49 C. del Cerro, J. M. García, A. Rojas, M. Tortajada, D. Ramón, B. Galán, M. A. Prieto and J. L. García, *J. Bacteriol.*, 2012, **194**, 5709-5710.
50 S. Vuilleumier, V. N. Khmelenina, F. Bringel, A. S. Reshetnikov, A. Lajus, S. Mangenot, Z. Rouy, H. J. M. Op den Camp, M. S. M. Jetten, A. A. Dispirito, P. Dunfield, M. G. Klotz, J. D. Semrau, L. Y. Stein, V. Barbe, C. Medigue, Y. A. Trotsenko and M. G. Kalyuzhnaya, *J. Bacteriol.*, 2012, **194**, 551-552.
51 L. Y. Stein, F. Bringel, A. A. DiSpirito, S. Han, M. S. M. Jetten, M. G. Kalyuzhnaya, K. D. Kits, M. G. Klotz, H. den Camp, J. D. Semrau, S. Vuilleumier, D. C. Bruce, J. F. Cheng, K. W. Davenport, L. Goodwin, S. S. Han, L. Hauser, A. Lajus, M. L. Land, A. Lapidus, S. Lucas, C. Médigue, S. Pitluck and T. Woyke, *J. Bacteriol.*, 2011, **193**, 2668-2669.
52 M. M. Svenning, A. G. Hestnes, I. Wartiainen, L. Y. Stein, M. G. Klotz, M. G. Kalyuzhnaya, A. Spang, F. Bringel, S. Vuilleumier, A. Lajus, C. Medigue, D. C. Bruce, J. F. Cheng, L. Goodwin, N. Ivanova, J. Han, C. S. Han, L. Hauser, B. Held, M. L. Land, A. Lapidus, S. Lucas, M. Nolan, S. Pitluck and T. Woyke, *J. Bacteriol.*, 2011, **193**, 6418-6419.
53 Y. Chen, A. Crombie, M. T. Rahman, S. N. Dedysh, W. Liesack, M. B. Stott, M. Alam, A. R. Theisen, J. C. Murrell and P. F. Dunfield, *J. Bacteriol.*, 2010, **192**, 3840-3841.
54 L. Y. Stein, S. Yoon, J. D. Semrau, A. A. DiSpirito, A. Crombie, J. C. Murrell, S. Vuilleumier, M. G. Kalyuzhnaya, H. J. Op den Camp, F. Bringel, D. Bruce, J. F. Cheng, A. Copeland, L. Goodwin, S. Han, L. Hauser, M. S. Jetten, A. Lajus, M. L. Land, A. Lapidus, S. Lucas, C. Médigue, S. Pitluck, T. Woyke, A. Zeytun and M. G. Klotz, *J. Bacteriol.*, 2010, **192**, 6497-6498.
55 N. Ward, O. Larsen, J. Sakwa, L. Bruseth, H. Khouri, A. S. Durkin, G. Dimitrov, L. Jiang, D. Scanlan, K. H. Kang, M. Lewis, K. E. Nelson, B. Methecute, M. Wu, J. F. Heidelberg, I. T. Paulsen, D. Fouts, J. Ravel, H. Tettelin, Q. Ren, T. Read, R. T. DeBoy, R. Seshadri, S. L. Salzberg, H. B. Jensen, N. K. Birkeland, W. C. Nelson, R. J. Dodson, S. H. Grindhaug, I. Holt, I. Eidhammer, I. Jonason, S. Vanaken, T. Utterback, T. V. Feldblyum, C. M. Fraser, J. R. Lillehaug and J. A. Eisen, *PLoS Biol.*, 2004, **2**, e303.
56 S. Stolyar, A. M. Costello, T. L. Peeples and M. E. Lidstrom, *Microbiol.*, 1999, **145**, 1235-1244.
57 J. D. Semrau, A. Chistoserdov, J. Lebron, A. Costello, J. Davagnino, E. Kenna, A. J. Holmes, R. Finch, J. C. Murrell and M. E. Lidstrom, *J. Bacteriol.*, 1995, **177**, 3071-3079.
58 I. R. McDonald and J. C. Murrell, *FEMS Microbiol. Lett.*, 1997, **156**, 205-210.
59 R. L. Lieberman and A. C. Rosenzweig, *Nature*, 2005, **434**, 177-182.
60 A. S. Hakemian, K. C. Kondapalli, J. Telser, B. M. Hoffman, T. L. Stemmler and A. C. Rosenzweig, *Biochemistry*, 2008, **47**, 6793-6801.
61 S. M. Smith, S. Rawat, J. Telser, B. M. Hoffman, T. L. Stemmler and A. C. Rosenzweig, *Biochemistry*, 2011, **50**, 10231-10240.
62 S. Sirajuddin, D. Barupala, S. Helling, K. Marcus, T. L. Stemmler and A. C. Rosenzweig, *J. Biol. Chem.*, 2014, **289**, 21782-21794.
63 S. Y. Ro, M. O. Ross, Y. W. Deng, S. Batelu, T. J. Lawton, J. D. Hurley, T. L. Stemmler, B. M. Hoffman and A. C. Rosenzweig, *J. Biol. Chem.*, 2018, **293**, 10457-10465.
64 J. Zhu, M. S. King, M. Yu, L. Klipcan, A. G. Leslie and J. Hirst, *Proc. Natl. Acad. Sci. USA*, 2015, **112**, 12087-12092.
65 J. A. Gerlt, J. T. Bouvier, D. B. Davidson, H. J. Imker, B. Sadkhin, D. R. Slater and K. L. Whalen, *Biochim. Biophys. Acta*, 2015, **1854**, 1019-1037.
66 D. J. Arp, L. A. Sayavedra-Soto and N. G. Hommes, *Arch. Microbiol.*, 2002, **178**, 250-255.
67 E. F. Liew, D. C. Tong, N. V. Coleman and A. J. Holmes, *Microbiology*, 2014, **160**, 1267-1277.
68 T. J. Lawton, J. Ham, T. Sun and A. C. Rosenzweig, *Proteins*, 2014, **82**, 2263-2267.
69 S. S. Lemos, M. L. P. Collins, S. S. Eaton, G. R. Eaton and W. E. Antholine, *Biophys. J.*, 2000, **79**, 1085-1094.
70 M. O. Ross, F. MacMillan, J. Wang, A. Nisthal, T. J. Lawton, B. D. Olafson, S. L. Mayo, A. C. Rosenzweig and B. M. Hoffman, *Science*, 2019, **364**, 566-570.
71 C. W. Koo and A. C. Rosenzweig, in *Encylopedia of Inorganic and Bioinorganic Chemistry*, John Wiley & Sons, Ltd., 2020, vol. DOI: 10.1002/9781119951438.eibc2740.
72 L. Ciano, G. J. Davies, W. B. Tolman and P. H. Walton, *Nat. Catal.*, 2018, **1**, 571-577.
73 P. H. Walton and G. J. Davies, *Curr. Opin. Chem. Biol.*, 2016, **31**, 195-207.
74 R. L. Lieberman, D. B. Shrestha, P. E. Doan, B. M. Hoffman, T. L. Stemmler and A. C. Rosenzweig, *Proc. Natl. Acad. Sci. USA*, 2003, **100**, 3820-3825.
75 R. L. Lieberman, K. C. Kondapalli, D. B. Shrestha, A. S. Hakemian, S. M. Smith, J. Telser, J. Kuzelka, R. Gupta, A. S. Borovik, S. J. Lippard, B. M. Hoffman, A. C. Rosenzweig and T. L. Stemmler, *Inorg. Chem.*, 2006, **45**, 8372-8381.
76 L. L. Cao, O. Caldararu, A. C. Rosenzweig and U. Ryde, *Angew. Chem. Int. Ed.*, 2018, **57**, 162-166.
77 S. Y. Ro, L. F. Schachner, C. W. Koo, R. Purohit, J. P. Remis, G. E. Kenney, B. W. Liauw, P. M. Thomas, S. M. Patrie, N. L. Kelleher and A. C. Rosenzweig, *Nat. Commun.*, 2019, **10**, 2675.
78 Y. Shiota, G. Juhasz and K. Yoshizawa, *Inorg. Chem.*, 2013, **52**, 7907-7917.
79 Y. Shiota and K. Yoshizawa, *Inorg. Chem.*, 2009, **48**, 838-845.
80 K. Yoshizawa and Y. Shiota, *J. Am. Chem. Soc.*, 2006, **128**, 9873-9881.
81 H. J. Kim, J. Huh, Y. W. Kwon, D. Park, Y. Yu, Y. E. Jang, B. R. Lee, E. Jo, E. J. Lee, Y. Heo, W. Lee and J. Lee, *Nat. Catal.*, 2019, **2**, 342-353.
82 G. Nyerges and L. Y. Stein, *FEMS Microbiol. Lett.*, 2009, **297**, 131-136.
83 L. Y. Stein and D. J. Arp, *Appl. Environ. Microbiol.*, 1998, **64**, 4098-4102.
84 N. V. Coleman, N. B. Le, M. A. Ly, H. E. Ogawa, V. McCarl, N. L. Wilson and A. J. Holmes, *Isme J.*, 2012, **6**, 171-182.
85 D. D. Smith and H. Dalton, *Eur. J. Biochem.*, 1989, **182**, 667-671.

86 A. K. Shiemke, S. A. Cook and T. Miley, *J. Inorg. Biochem.*, 1995, **59**, 385.
87 H. Heinrich and S. Werner, *Biochemistry*, 1992, **31**, 11413-11419.
88 S. A. Cook and A. K. Shiemke, *Arch. Biochem. Biophys.*, 2002, **398**, 32-40.
89 A. de la Torre, A. Metivier, F. Chu, L. M. L. Laurens, D. A. C. Beck, P. T. Pienkos, M. E. Lidstrom and M. G. Kalyuzhnaya, *Microb. Cell Fact.*, 2015, **14**, 188.
90 D. J. Leak and H. Dalton, *Appl. Microbiol. Biotechnol.*, 1986, **23**, 477-481.
91 C. Lieven, L. A. H. Petersen, S. B. Jorgensen, K. V. Gernaey, M. J. Herrgard and N. Sonnenschein, *Front. Microbiol.*, 2018, **9**, 15.
92 S. Bordel, Y. Rodriguez, A. Hakobyan, E. Rodriguez, R. Lebrero and R. Munoz, *Metab. Eng.*, 2019, **54**, 191-199.
93 S. Bordel, A. Rojas and R. Munoz, *Microb. Cell Fact.*, 2019, **18**, 11.
94 A. D. Nguyen, J. Y. Park, I. Y. Hwang, R. Hamilton, M. G. Kalyuzhnaya, D. Kim and E. Y. Lee, *Metab. Eng.*, 2020, **57**, 1-12.
95 S. Naizabekov and E. Y. Lee, *Microorganisms*, 2020, **8**, 19.
96 N. Myronova, A. Kitmitto, R. F. Collins, A. Miyaji and H. Dalton, *Biochemistry*, 2006, **45**, 11905-11914.
97 M. A. Culpepper and A. C. Rosenzweig, *Biochemistry*, 2014, **53**, 6211-6219.
98 Y. W. Deng, S. Y. Ro and A. C. Rosenzweig, *J. Biol. Inorg. Chem.*, 2018, **23**, 1037-1047.
99 O. S. Fisher, G. E. Kenney, M. O. Ross, S. Y. Ro, B. E. Lemma, S. Batelu, P. M. Thomas, V. C. Sosnowski, C. J. DeHart, N. L. Kelleher, T. L. Stemmler, B. M. Hoffman and A. C. Rosenzweig, *Nat. Commun.*, 2018, **9**, 4276.
100 M. O. Ross, O. S. Fisher, M. N. Morgada, M. D. Krzyaniak, M. R. Wasielewski, A. J. Vila, B. M. Hoffman and A. C. Rosenzweig, *J. Am. Chem. Soc.*, 2019, **141**, 4678-4686.
101 J. C. Murrell, *Biodeg.*, 1994, **5**, 145-159.
102 S.-K. Lee, J. C. Nesheim and J. D. Lipscomb, *J. Biol. Chem.*, 1993, **268**, 21569-21577.
103 Y. Liu, J. C. Nesheim, S. K. Lee and J. D. Lipscomb, *J. Biol. Chem.*, 1995, **270**, 24662-24665.
104 M. Merkx and S. J. Lippard, *J. Biol. Chem.*, 2002, **277**, 5858-5865.
105 M. H. Sazinsky, M. Merkx, E. Cadieux, S. Y. Tang and S. J. Lippard, *Biochemistry*, 2004, **43**, 16263-16276.
106 A. C. Rosenzweig, C. A. Frederick, S. J. Lippard and P. Nordlund, *Nature*, 1993, **366**, 537-543.
107 N. Elango, R. Radhakrishnan, W. A. Froland, B. J. Wallar, C. A. Earhart, J. D. Lipscomb and D. H. Ohlendorf, *Protein Sci.*, 1997, **6**, 556-568.
108 A. C. Rosenzweig, P. Nordlund, P. M. Takahara, C. A. Frederick and S. J. Lippard, *Chem. Biol.*, 1995, **2**, 409-418.
109 V. Srinivas, R. Banerjee, H. Lebrette, J. C. Jones, O. Aurelius, I. S. Kim, C. C. Pham, S. Gul, K. Sutherlin, A. Bhowmick, J. John, E. Bozkurt, T. Fransson, P. Aller, A. Butryn, I. Bogacz, P. S. Simon, S. Keable, A. Britz, K. Tono, K. S. Kim, S. Y. Park, S. J. Lee, J. Park, R. Alonso-Mori, F. Fuller, A. Batyuk, A. Brewster, U. Bergmann, N. Sauter, A. M. Orville, V. K. Yachandra, J. Yano, J. D. Lipscomb, J. F. Kern and M. Hogbom, *J. Am. Chem. Soc.*, 2020, **142**, 14249-14266.
110 K. J. Walters, G. T. Gassner, S. J. Lippard and G. Wagner, *Proc. Natl. Acad. Sci. USA*, 1999, **96**, 7877-7882.
111 S. L. Chang, B. J. Wallar, J. D. Lipscomb and K. H. Mayo, *Biochemistry*, 1999, **38**, 5799-5812.
112 J. Müller, A. A. Lugovskoy, G. Wagner and S. J. Lippard, *Biochemistry*, 2002, **41**, 42-51.
113 L. L. Chatwood, J. Muller, J. D. Gross, G. Wagner and S. J. Lippard, *Biochemistry*, 2004, **43**, 11983-11991.
114 S. J. Lee, M. S. McCormick, S. J. Lippard and U.-S. Cho, *Nature*, 2013, **494**, 380-384.
115 H. Kim, S. An, Y. R. Park, H. Jang, H. Yoo, S. H. Park, S. J. Lee and U. S. Cho, *Sci Adv*, 2019, **5**, eaax0059.
116 W. X. Wang, R. E. Iacob, R. P. Luoh, J. R. Engen and S. J. Lippard, *J. Am. Chem. Soc.*, 2014, **136**, 9754-9762.
117 D. A. Kopp, E. A. Berg, C. E. Costello and S. J. Lippard, *J. Biol. Chem.*, 2003, **278**, 20939-20945.
118 B. G. Fox, Y. Liu, J. E. Dege and J. D. Lipscomb, *J. Biol. Chem.*, 1991, **266**, 540-550.
119 Y. Liu, J. C. Nesheim, K. E. Paulsen, M. T. Stankovich and J. D. Lipscomb, *Biochemistry*, 1997, **36**, 5223-5233.
120 J. F. Acheson, L. J. Bailey, N. L. Elsen and B. G. Fox, *Nat Commun*, 2014, **5**, 5009.
121 K. E. Liu and S. J. Lippard, *J. Biol. Chem.*, 1991, **266**, 12836-12839, 24859.
122 K. E. Paulsen, Y. Liu, B. G. Fox, J. D. Lipscomb, E. Münck and M. T. Stankovich, *Biochemistry*, 1994, **33**, 713-722.
123 B. J. Brazeau, B. J. Wallar and J. D. Lipscomb, *Biochem. Biophys. Res. Commun.*, 2003, **312**, 143-148.
124 A. Ericson, B. Hedman, K. O. Hodgson, J. Green, H. Dalton, J. G. Bentsen, R. H. Beer and S. J. Lippard, *J. Am. Chem. Soc.*, 1988, **110**, 2330.
125 B. G. Fox, K. K. Surerus, E. Münck and J. D. Lipscomb, *J. Biol. Chem.*, 1988, **263**, 10553-10556.
126 W. Wang, A. D. Liang and S. J. Lippard, *Acc. Chem. Res.*, 2015, **48**, 2632-2639.
127 D. A. Whittington, A. C. Rosenzweig, C. A. Frederick and S. J. Lippard, *Biochemistry*, 2001, **40**, 3476-3482.
128 M. H. Sazinsky and S. J. Lippard, *J. Am. Chem. Soc.*, 2005, **127**, 5814-5825.
129 B. J. Wallar and J. D. Lipscomb, *Biochemistry*, 2001, **40**, 2220-2233.
130 B. J. Brazeau and J. D. Lipscomb, *Biochemistry*, 2003, **42**, 5618-5631.
131 J. C. Jones, R. Banerjee, K. Shi, H. Aihara and J. D. Lipscomb, *Biochemistry*, 2020, **59**, 2946-2961.
132 A. J. Jasniewski and L. Que, Jr., *Chem. Rev.*, 2018, **118**, 2554-2592.
133 K. E. Liu, A. M. Valentine, D. Qiu, D. E. Edmondson, E. H. Appelman, T. G. Spiro and S. J. Lippard, *J. Am. Chem. Soc.*, 1995, **117**, 4987-4990.
134 S.-K. Lee and J. D. Lipscomb, *Biochemistry*, 1999, **38**, 4423-4432.
135 C. E. Tinberg and S. J. Lippard, *Biochemistry*, 2009, **48**, 12145-12158.
136 R. Banerjee, K. K. Meier, E. Münck and J. D. Lipscomb, *Biochemistry*, 2013, **52**, 4331-4342.
137 S.-K. Lee, B. G. Fox, W. A. Froland, J. D. Lipscomb and E. Münck, *J. Am. Chem. Soc.*, 1993, **115**, 6450-6451.
138 K. E. Liu, A. M. Valentine, D. Wang, B. H. Huynh, D. E. Edmondson, A. Salifoglou and S. J. Lippard, *J. Am. Chem. Soc.*, 1995, **117**, 10174-10185.
139 R. Banerjee, Y. Proshlyakov, J. D. Lipscomb and D. A. Proshlyakov, *Nature*, 2015, **518** 431-434.
140 R. G. Castillo, R. Banerjee, C. J. Allpress, G. T. Rohde, E. Bill, L. Que, J. D. Lipscomb and S. DeBeer, *J. Am. Chem. Soc.*, 2017, **139**, 18024-18033.
141 L. Shu, J. C. Nesheim, K. Kauffmann, E. Münck, J. D. Lipscomb and L. Que, Jr., *Science*, 1997, **275**, 515-518.

142 G. E. Cutsail, III, R. Banerjee, A. Zhou, L. Que, Jr., J. D. Lipscomb and S. DeBeer, *J. Am. Chem. Soc.*, 2018, **140**, 16807-16820.
143 G. Xue, R. De Hont, E. Münck and L. Que, Jr., *Nature chemistry*, 2010, **2**, 400-405.
144 B. F. Gherman, S. J. Lippard and R. A. Friesner, *J. Am. Chem. Soc.*, 2005, **127**, 1025-1037.
145 S. P. Huang, Y. Shiota and K. Yoshizawa, *Dalton Trans.*, 2013, **42**, 1011-1023.
146 K. J. Burrows, A. Cornish, D. Scott and I. J. Higgins, *J. Gen. Microbiol.*, 1984, **130**, 327-3333.
147 J. Green and H. Dalton, *J. Biol. Chem.*, 1989, **264**, 17698-17703.
148 J. Colby, D. I. Stirling and H. Dalton, *Biochem. J.*, 1977, **165**, 395-402.
149 N. D. Priestley, H. G. Floss, W. A. Froland, J. D. Lipscomb, P. G. Williams and H. Morimoto, *J. Am. Chem. Soc.*, 1992, **114**, 7561-7562.
150 A. M. Valentine, B. Wilkinson, K. E. Liu, S. Komar-Panicucci, N. D. Priestley, P. G. Williams, H. Morimoto, H. G. Floss and S. J. Lippard, *J. Am. Chem. Soc.*, 1997, **119**, 1818-1827.
151 K. E. Liu, C. C. Johnson, M. Newcomb and S. J. Lippard, *J. Amer. Chem. Soc.*, 1993, **115**, 939-947.
152 Y. Jin and J. D. Lipscomb, *Biochemistry*, 1999, **38**, 6178-6186.
153 A. M. Valentine, M. H. LeTadic-Biadatti, P. H. Toy, M. Newcomb and S. J. Lippard, *J. Biol. Chem.*, 1999, **274**, 10771-10776.
154 B. J. Brazeau, R. N. Austin, C. Tarr, J. T. Groves and J. D. Lipscomb, *J. Am. Chem. Soc.*, 2001, **123**, 11831-11837.
155 J. C. Nesheim and J. D. Lipscomb, *Biochemistry*, 1996, **35**, 10240-10247.
156 B. J. Brazeau, B. J. Wallar and J. D. Lipscomb, *J. Am. Chem. Soc.*, 2001, **123**, 10421-10422.
157 C. A. Brantner, C. C. Remsen, H. A. Owen, L. A. Buchholz and M. L. P. Collins, *Arch. Microbiol.*, 2002, **178**, 59-64.
158 V. Cafaro, V. Izzo, R. Scognamiglio, E. Notomista, P. Capasso, A. Casbarra, P. Pucci and A. Di Donato, *Appl. Environ. Microbiol.*, 2004, **70**, 2211-2219.
159 J. D. Pikus, J. M. Studts, C. Achim, K. E. Kauffmann, E. Münck, R. J. Steffan, K. McClay and B. G. Fox, *Biochemistry*, 1996, **35**, 9106-9119.
160 T. J. Smith and J. C. Murrell, *Methods Enzymol.*, 2011, **495**, 135-147.
161 T. J. Smith and T. Nichol, in *Methane Biocatalysis: Paving the Way to Sustainability*, eds. M. G. Kalyuzhnaya and X.-H. Xing, Springer International Publishing, Cham, 2018, DOI: 10.1007/978-3-319-74866-5_10, pp. 153-168.
162 E. Borodina, T. Nichol, M. G. Dumont, T. J. Smith and J. C. Murrell, *Appl. Environ. Microbiol.*, 2007, **73**, 6460-6467.
163 M. Lock, T. Nichol, J. C. Murrell and T. J. Smith, *FEMS Microbiol. Lett.*, 2017, **364**, fnx137.
164 F. D. Orata, J. P. Meier-Kolthoff, D. Sauvageau and L. Y. Stein, *Front. Microbiol.*, 2018, **9**, 3162.
165 A. W. Puri, S. Owen, F. Chu, T. Chavkin, D. A. C. Beck, M. G. Kalyuzhnaya and M. E. Lidstrom, *Appl. Environ. Microbiol.*, 2015, **81**, 1766-1772.
166 X. Yan, F. Chu, A. W. Puri, Y. F. Fu and M. E. Lidstrom, *Appl. Environ. Microbiol.*, 2016, **82**, 2062-2069.
167 T. Tapscott, M. T. Guarnieri and C. A. Henard, *Appl. Environ. Microbiol.*, 2019, **85**, e00340-00319.